

1 Accepted at BMJ Open Ophthalmology

2 **Assessment of local sensitivity in incomplete retinal-pigment-epithelium and**  
3 **outer retinal atrophy (iRORA) lesions in intermediate age-related macular**  
4 **degeneration (iAMD)**

5 Julius Ameln, M.Sc.<sup>1\*</sup>; Marlene Saßmannshausen, MD<sup>1\*</sup>; Leon von der Emde, MD<sup>1\*</sup>; Alessandra  
6 Carmichael-Martins, PhD<sup>1</sup>; Frank G. Holz, MD<sup>1</sup>; Thomas Ach, MD <sup>1</sup>; Wolf M. Harmening, PhD<sup>1</sup>

7 <sup>1</sup>Department of Ophthalmology, University Hospital Bonn, Germany

8 \*J. Ameln, M. Saßmannshausen and L. von der Emde contributed equally and should be  
9 considered shared first authors.

10

11 *Key words:* AMD, geographic atrophy, precursor lesion, retinal function,  
12 microperimetry, adaptive optics, AOSLO-MP, clinical outcome measures

13

14 *Number of words:* 252 + 886 + 291 + 415 + 50 = 1894

15 *Number of color figures:* 2

16 *Number of tables:* 1

17 *Number of supplemental figures:* None

18 *Corresponding Author:*

19 Wolf M. Harmening, PhD

20 Department of Ophthalmology

21 University Eye Hospital Bonn

22 Venusberg-Campus 1

23 53127 Bonn - Germany

24 Tel.: +49 228 287 15882

25 e-mail: wolf.harmening@ukbonn.de

26 **ABSTRACT**

27 Lesions of incomplete retinal-pigment-epithelium and outer retinal atrophy (iRORA) are  
28 associated with disease progression in age-related macular degeneration (AMD). However, the  
29 corresponding functional impact of these precursor lesions is unknown.

30 We present a cross-sectional study of four patients employing clinical-grade MAIA (stimulus  
31 size:  $0.43^\circ$ ,  $\sim 125 \mu\text{m}$ ) and adaptive optics scanning light ophthalmoscope (AOSLO, stimulus  
32 size  $0.07^\circ$ ,  $\sim 20 \mu\text{m}$ ) based microperimetry (MP) to assess the specific impact of iRORA lesions  
33 on retinal sensitivity.

34 AOSLO imaging showed overall reduced photoreceptor reflectivity and patches of hyporeflective  
35 regions at drusen with interspersed hyperreflective foci in iRORA regions. MAIA-MP yielded an  
36 average retinal sensitivity loss of  $-7.3 \pm 3.1$  dB at iRORA lesions compared to the in-eye control.  
37 With AOSLO-MP, the corresponding sensitivity loss was  $-20.1 \pm 4.8$  dB.

38 We demonstrated that iRORA lesions are associated with a severe impairment in retinal  
39 sensitivity. Larger cohort studies will be necessary to validate our findings.

## 40 INTRODUCTION

41 There is an unmet need for prognostic biomarkers and clinical endpoints, approved by  
42 regulatory authorities, in early and intermediate age-related macular degeneration (AMD).[1] In  
43 recent years, high-resolution multimodal retinal imaging, including spectral domain optical  
44 coherence tomography (SD-OCT), has identified precursor lesions of geographic atrophy (GA)  
45 in AMD.[2] These have been further characterized by the International Consensus Atrophy  
46 Meeting (CAM) group and termed as incomplete retinal-pigment-epithelium and outer retinal  
47 atrophy (iRORA) in SD-OCT imaging, preceding its later stage, complete RPE and outer retinal  
48 atrophy, cRORA.[3] While iRORA is highly associated with disease progression,[4] detailed  
49 knowledge of its impact on retinal function is very limited, yet essential for its validation as a  
50 potential clinical outcome measure. Conventional functional tests such as microperimetry (MP)  
51 are inadequate due to the discrepancy between available test stimuli sizes and the tiny iRORA  
52 lesion sizes.

53 Nowadays, adaptive optics scanning light ophthalmoscope (AOSLO) imaging allows cell  
54 resolved visualization of photoreceptors by correcting the human eyes natural aberrations.[5]  
55 AOSLO systems have been further adapted to allow AOSLO-MP, utilizing the high resolution of  
56 the system to facilitate functional sensitivity testing of small retinal areas down to the size of  
57 individual photoreceptors.[6–8] AOSLO-MP has helped to investigate the functional relevance of  
58 retinal phenotypes in various diseases, including Macular telangiectasia type 2, Choroideremia  
59 and Retinitis pigmentosa.[9–11]

60 The purpose of this cross-sectional study is to juxtapose retinal sensitivity, gauged through  
61 clinical-grade MP and AOSLO-MP, at retinal locations in presence and absence of iRORA to  
62 determine the lesions' impact on retinal function.

## 63 **METHODS**

64

### 65 **Patients**

66 For this study, patients with large sub-RPE drusen ( $\geq 125 \mu\text{m}$ ) associated with iAMD according  
67 to the Beckman classification [12] and at least one iRORA [3] lesion (region of choroidal  
68 hypertransmission  $< 250 \mu\text{m}$ , zone of attenuation/disruption of the RPE  $< 250 \mu\text{m}$ , evidence of  
69 overlying photoreceptor degeneration in absence of an RPE tear) were recruited. Exclusion  
70 criteria were any history of other retinal diseases, glaucoma, previous history of vitreoretinal  
71 surgery, relevant anterior segment disease with media opacity, cRORA or a history of current or  
72 previous anti-VEGF treatment. If both eyes of a study patient had iRORA, the eye with a more  
73 extrafoveal position of the lesion as well as better BCVA was chosen as study eye. All patients  
74 underwent routine ophthalmological examination including best-corrected visual acuity (BCVA),  
75 slit lamp and funduscopic examination. Following pupil dilation (0.5% tropicamide, 2.5%  
76 phenylephrine), a standardized retinal imaging protocol was performed using SD-OCT raster  
77 scanning (241 B-scans,  $30^\circ \times 25^\circ$  enhanced-depth-imaging [EDI] mode, centered on the fovea,  
78 lateral scan distance  $30 \mu\text{m}$ , automatic real-time mode 9 frames; Spectralis, Heidelberg  
79 Engineering, Heidelberg, Germany). Throughout this study, a retinal magnification factor of  $291$   
80  $\mu\text{m}/\text{deg}$  of visual angle was assumed.

81 All patients were recruited at the University Eye Hospital Bonn, Germany, and written informed  
82 consent was obtained after explanation of the study's nature and possible consequences. The  
83 study was approved by the institutional Ethics committee (#125/14 & #009/13) and was  
84 conducted in accordance with the tenets of the Declaration of Helsinki.

85

### 86 **iRORA grading**

87 For precise localization of iRORA, each B-scan of the 241-volume SD-OCT scan was screened

88 by two medical expert graders (MS, LvDE) with specific expertise in iAMD trials. The largest  
89 horizontal diameter of the lesion was annotated within the B-scan. For MP testing, in eye control  
90 regions were chosen by eccentricity-matching via mirroring along the foveal vertical meridian.  
91 Control regions were allowed to present iAMD-typical structural alterations but required to not  
92 contain any iRORA lesions or large blood vessels. In case the requirements were not met, the  
93 control region was shifted horizontally or vertically to a valid retinal region, which was found in  
94 all cases by shifting less than 100  $\mu\text{m}$  from the initially targeted area. The targeted area was  
95 generally smaller than 250  $\mu\text{m}$  edge length, centered on the lesion crossing central B-scan. Per  
96 eye, a single iRORA lesion and a single in-eye control region was examined with clinical-grade  
97 (MAIA-) and AOSLO-MP. Fundus images showing the MP target locations and AOSLO images  
98 of the respective regions are shown in Figure 1.

99

#### 100 **MAIA-MP**

101 For clinical-grade retinal sensitivity testing, the S-MAIA device (CenterVue/iCare, Padova, Italy)  
102 was employed (settings: 85 stimuli covering  $12^\circ$  of the central retina, 4-2 dB staircase strategy,  
103 stimulus size:  $0.43^\circ$  [Goldmann III]). An initial training session was performed in all patients prior  
104 to the main test using achromatic stimuli (400–800 nm). The MAIA test duration was about 8-10  
105 minutes. The MAIA background luminance was 4 apostilb (asb, or  $1.3 \text{ cd/m}^2$ ) with a dynamic  
106 testing range of 36 dB. The MAIA grid stimulation pattern was aligned according to vessel  
107 bifurcations to the en-face IR of the SD-OCT image using Fiji, Image J (U.S. National Institutes  
108 of Health). Under detailed consideration of the corresponding OCT B-scans, the MAIA stimuli  
109 points at the position of the respective iRORA lesion were identified.

110

#### 111 **AOSLO-MP**

112 A custom dual channel confocal AOSLO was used to simultaneously image the retina

113 (wavelength 840 nm; field of view: 0.85°) and to deliver visual stimuli at 543 nm (test spot  
114 diameter: 0.07°).[7] The custom AOSLO-MP instrument has been described previously in  
115 detail.[7] In summary, the setup comprised a broadband laser source (SuperK EXTREME; NKT  
116 Photonics, Birkerød, Denmark) that was used to provide multiple light channels. The integrated  
117 adaptive optics consisted of a Shack-Hartmann wavefront sensor (SHSCam AR-S-150-GE;  
118 Optocraft GmbH, Erlangen, Germany) and a deformable mirror (DM97-08; ALPAO,  
119 Montbonnot-Saint-Martin, France) in closed loop. Wavefront sensing was performed using the  
120 imaging wavelength. Two acousto-optic modulators (TEM-250-50-10-2FP; Brimrose, Sparks  
121 Glencoe, MD, USA) in cascaded configuration allowed generation of high-contrast visual stimuli  
122 at a wavelength of 543 nm.[7, 8] The 840 nm AOSLO imaging field created a constant  
123 background illumination of 13.2 asb (4.2 cd/m<sup>2</sup>) against which the 543 nm test spots were  
124 shown. Visual stimuli could be presented over a 50 dB dynamic range.[7, 8]

125 The position of the patients' head was controlled using a dental impression stage (bite bar).  
126 Patients were instructed to fixate on a small visual annulus presented via a pellicle beam splitter  
127 during imaging and testing. A 4-2 dB descending staircase strategy with three threshold  
128 crossings was used. Sensitivity thresholds at both iRORA and control test sites were defined in  
129 dB as the average from at least 5 valid repeat runs per location (5 at iRORA, 5 at control  
130 region). Runs where catch and lapse trials were notable, or where the patient or the supervisor  
131 noted down any issue, were excluded from the analyses. Prior to testing, AOSLO images were  
132 recorded at the relevant retinal locations. Patients then performed several practice runs to  
133 familiarize themselves with the test procedure. While each single AOSLO-MP test run took less  
134 than a minute to complete, the total time for AOSLO imaging and AOSLO-MP took about 1 hour  
135 per eye.

136

137 **Statistical Analysis**

138 A one-sided two-sample t-test was carried out using the *ttest2* Matlab function to test for  
139 statistical significance ( $p < 0.05$ ) of AOSLO-MP sensitivity loss in presence and absence of  
140 iRORA.

141 **RESULTS**

142 Four eyes of four iAMD patients (mean age: 73, range: 60 - 85) were included. Detailed patient  
 143 characteristics are given in **Table 1**. Multimodal imaging of iRORA and control regions is shown  
 144 in **Figure 1**. When averaged across all four test eyes, the loss of sensitivity at the iRORA site  
 145 relative to the control site was  $20.1 \pm 4.8$  dB for AOSLO-MP and  $7.3 \pm 3.1$  dB for MAIA-MP  
 146 (**Figure 2**).

147 **Table 1:**

Patient	Sex	Eye	Lens status	BCVA [logMAR]	MAIA-MP threshold [dB]		AOSLO-MP threshold [dB]	
					iRORA	control	iRORA	control
# 1	f	OD	Phakic	-0.1	21	25	$9.4 \pm 1.2$	$34.7 \pm 0.4$
# 2	m	OD	Phakic	0.1	-	-	$12.6 \pm 4.1$	$28.4 \pm 2.6$
# 3	f	OS	Phakic	0.0	17	27	$14.0 \pm 3.0$	$33.3 \pm 2.2$
# 4	f	OD	Pseudophakic	0.4	13	21	-	-

148 **Table 1: Patient ocular characteristics and retinal sensitivity thresholds.** If available,  
 149 averages  $\pm$  one standard deviation are reported. **Abbreviations:** BCVA = Best corrected visual  
 150 acuity, logMAR = Logarithm of the minimum angle of resolution, MP = Microperimetry, dB =  
 151 Decibel. AOSLO = Adaptive optics scanning light ophthalmoscope. MAIA-MP was not available  
 152 in patient #3, AOSLO-MP was not available in patient #4.

154 **Selected cases**

155 Patient #1 presented with hyperreflective material and hyporefective patches at the  
 156 photoreceptor level at the iRORA lesion, surrounded by structurally altered photoreceptors. The  
 157 control region showed an irregular photoreceptor mosaic with large patches of slightly  
 158 hyporefective photoreceptors (**Figure 1**). AOSLO-MP revealed a retinal sensitivity threshold of  
 159  $9.4$  dB at the iRORA lesion and of  $34.7$  dB ( $25.3$  dB difference,  $p < 0.01$  two-sample t-test) at the  
 160 control region (**Figure 2**). The corresponding MAIA-MP sensitivity difference was  $4$  dB.



161 Patient #2 iRORA lesion and control region displayed morphologies similar to Patient #1.  
162 AOSLO-MP was successful, showing a significant retinal sensitivity loss between iRORA lesion  
163 and control region (15.8 dB,  $p < 0.01$ ), while MAIA-MP failed due to patient fatigue (Table 1,  
164 Figure 2).

165 Patient #3 displayed patches of healthy-appearing photoreceptors surrounded by less reflective  
166 and irregularly arranged photoreceptors, as well as regions of hyporeflexive photoreceptors, at  
167 the location of the iRORA lesion. The respective control region had a similar appearance  
168 (**Figure 1**). AOSLO-MP revealed a sensitivity loss of 19.3 dB between iRORA and control  
169 ( $p < 0.01$ ), the MAIA-MP sensitivity loss was 10 dB (**Figure 2**).

170 Patient #4 iRORA lesion appeared as a central black area surrounded by remnant enlarged  
171 cone structures. AOSLO-MP failed due to insufficient fixation stability of the patient. MAIA-MP  
172 showed a significant retinal sensitivity loss between the iRORA lesion and control region (8 dB,  
173  $p < 0.01$ ) Table 1, Figure 2).

174

175 **DISCUSSION**

176 We here report the immediate impact of iRORA lesions on retinal function in four patients with  
177 iAMD. iRORA is a structural precursor for GA development but can now also be linked to  
178 functional impairments detected by AOSLO-MP.

179 The image signal in confocal AOSLO stems from the reflective properties of the photoreceptors'  
180 outer segments. Patches of less reflective and irregularly arranged photoreceptors, as seen in  
181 our patients, are thus highly suspicious of functional and structural impairment. Specifically, the  
182 displacement of the cells i.e. by drusen, as well damage to the outer segments are likely causes  
183 of the observed changes. The photoreceptor mosaic phenotype at iRORA lesions here reported  
184 (see Figure 1), seems to be comparable to previously reported structural changes at retinal  
185 locations with iAMD drusen (patient #3) or GA (patient #4).[13, 14] Interestingly, while all iRORA  
186 lesions showed abnormalities in photoreceptor arrangement and reflectivity, the impact on  
187 function differed across patients. It is hypothesized that with iRORA progression, photoreceptors  
188 will further deteriorate. However, photoreceptor loss in areas of iRORA cannot be readily  
189 quantified and compared to control regions by confocal AOSLO, given the impact of  
190 photoreceptor outer segment health changes on this imaging modality.

191 In all our patients, a significant loss of retinal sensitivity at the iRORA lesions was detectable.  
192 While both MAIA-MP and AOSLO-MP results demonstrate functional loss, its magnitude is  
193 about 4 times higher in AOSLO-MP, on average. We suggest that this difference is explained by  
194 the smaller and finely targeted stimulus available for AOSLO-MP. The ~6 times larger  
195 Goldmann 3 stimulus used for MAIA-MP likely includes areas not affected by the small iRORA  
196 lesions and elicits retinal responses by comparably healthy adjacent photoreceptors (compare  
197 patient #1 and #3). The steep retinal sensitivity loss detected with AOSLO-MP indicates that  
198 iRORA lesions can be considered as a surrogate marker for retinal dysfunction. A Limitation of  
199 our study is the fundamentally different setup of the MAIA-MP and AOSLO-MP. The AOSLO-

200 MP background illumination is about 3.3 times brighter due to light requirements of the adaptive  
201 optics components used for wavefront correction and retinal imaging. Furthermore, the MAIA-  
202 MP uses white stimuli, while green (543 nm center wavelength) stimuli are used for AOSLO-MP,  
203 selected for equal sensitivity in the long- and middle-wavelength sensitive cones. Additionally,  
204 we have a small shared patient pool. One patient failed the MAIA-MP (patient fatigue), and one  
205 failed the ASLO-MP (insufficient fixation stability), resulting in only 2 patients with shared results  
206 for both MAIA-MP and AOSLO-MP out of a total of 4 recruited patients.

207

## 208 **CONCLUSIONS**

209 This pilot study revealed a statistically significant and severe decrease in retinal sensitivity at  
210 iRORA lesions in iAMD patients. Larger cohort studies will be necessary to validate our findings.

211

212

213

214

215

216

217

218

219

220

221

222

223

224 **ACKNOWLEDGEMENT SECTION**

225

226 **Funding**

227 This work was supported by the Fem Habil Program, Faculty of Medicine, University of Bonn,  
228 Germany to MS, the Jackstaedt Foundation to LvdE, by the NIH/NEI (Grant No 1R01EY027948)  
229 to TA and by the German Research Foundation (DFG, Grant No HA 5323/6-1) to WH.

230

231 **Role of the funder**

232 The funding organization had no role in the design or conduct of the study.

233

234 **Acknowledgements**

235 The authors thank the patients for participating in the study. The authors further thank Aleksandr  
236 Gutnikov for his software support.

237

238 **Competing interests**

239 J. Ameln: none

240 M. Saßmannshausen: Heidelberg Engineering (F), CenterVue (F), Carl Zeiss MedicTec (F).

241 L. Von der Emde: Heidelberg Engineering (F), CenterVue (F), Carl Zeiss MedicTec (F).

242 T. Ach: Bayer (C), Roche (C), Novartis (C), Novartis (R), Heidelberg Engineering (C), Apellis  
243 Pharmaceuticals (C), Nidek (C, R).

244 F.G. Holz: Acucela (C, F), Allergan (F), Apellis (C, F), Bayer (C, F), Boehringer-Ingelheim (C),  
245 Bioeq/Formycon (F, C), CenterVue (F), Ellex (F), Roche/Genentech (C, F), Geuder (C, F),  
246 Graybug (C), Gyroscope (C), Heidelberg Engineering (C, F), IvericBio (C, F), Kanghong (C, F),  
247 LinBioscience (C), NightStarX (F), Novartis (C, F), Optos (F), Oxurion (C), Pixium Vision (C, F),  
248 Oxurion (C), Stealth BioTherapeutics (C), Zeiss (F, C).

249 W. Harmening: none

250

251

252 **Ethics approval**

253 The study was approved by the institutional Ethics committee (#125/14 & #009/13) of the  
254 University of Bonn.

255

256 **Contributorship**

257 All authors conceived the study. FGH, TA and WMH provided the devices used in the study. JA,  
258 MS and LvdE conducted the study. JA, MS and LvdE analyzed the results and wrote the  
259 manuscript. JA, LvdE and WMH created the figures. All authors discussed the results and  
260 revised the manuscript. WMH is the guarantor and responsible for the overall content of the  
261 study.

262

263 **Prior presentation**

264 Part of this work has previously been presented at the Classification of Atrophy Meeting (CAM)  
265 2023.

266

267

268

269

270

271

272

273

274

275

276

277

278 REFERENCES

- 279 1 Fleckenstein M, Keenan TDL, Guymer RH, et al. Age-related macular degeneration. *Nat Rev Dis*  
280 *Primers* 2021;7(1):31. doi:10.1038/s41572-021-00265-2 [published Online First: 6 May 2021].
- 281 2 Holz FG, Sadda SR, Staurengi G, et al. Imaging Protocols in Clinical Studies in Advanced Age-  
282 Related Macular Degeneration: Recommendations from Classification of Atrophy Consensus  
283 Meetings. *Ophthalmology* 2017;124(4):464–78. doi:10.1016/j.ophtha.2016.12.002 [published  
284 Online First: 18 January 2017].
- 285 3 Guymer RH, Rosenfeld PJ, Curcio CA, et al. Incomplete Retinal Pigment Epithelial and Outer Retinal  
286 Atrophy in Age-Related Macular Degeneration: Classification of Atrophy Meeting Report 4.  
287 *Ophthalmology* 2020;127(3):394–409. doi:10.1016/j.ophtha.2019.09.035 [published Online First:  
288 30 September 2019].
- 289 4 Wu Z, Goh KL, Hodgson LAB, et al. Incomplete Retinal Pigment Epithelial and Outer Retinal  
290 Atrophy: Longitudinal Evaluation in Age-Related Macular Degeneration. *Ophthalmology*  
291 2023;130(2):205–12. doi:10.1016/j.ophtha.2022.09.004 [published Online First: 11 September  
292 2022].
- 293 5 Roorda A, Romero-Borja F, Donnelly Iii W, et al. Adaptive optics scanning laser ophthalmoscopy.  
294 *Opt Express* 2002;10(9):405–12.
- 295 6 Tuten WS, Tiruveedhula P, Roorda A. Adaptive optics scanning laser ophthalmoscope-based  
296 microperimetry. *Optom Vis Sci* 2012;89(5):563–74.
- 297 7 Domdei N, Domdei L, Reiniger JL, et al. Ultra-high contrast retinal display system for single  
298 photoreceptor psychophysics. *Biomed Opt Express* 2018;9(1):157–72.
- 299 8 Domdei N, Reiniger JL, Holz FG, et al. The Relationship Between Visual Sensitivity and Eccentricity,  
300 Cone Density and Outer Segment Length in the Human Foveola. *Invest. Ophthalmol. Vis. Sci.*  
301 2021;62(9):31.
- 302 9 Foote KG, Wong JJ, Boehm AE, et al. Comparing Cone Structure and Function in RHO- and RPGR-  
303 Associated Retinitis Pigmentosa. *Invest Ophthalmol Vis Sci* 2020;61(4):42.
- 304 10 Tuten WS, Vergilio GK, Young GJ, et al. Visual function at the atrophic border in choroideremia  
305 assessed with adaptive optics microperimetry. *Ophthalmology Retina* 2019.
- 306 11 Wang Q, Tuten WS, Lujan BJ, et al. Adaptive optics microperimetry and OCT images show  
307 preserved function and recovery of cone visibility in macular telangiectasia type 2 retinal lesions.  
308 *Invest Ophthalmol Vis Sci* 2015;56(2):778–86.
- 309 12 Ferris FL, Wilkinson CP, Bird A, et al. Clinical classification of age-related macular degeneration.  
310 *Ophthalmology* 2013;120(4):844–51. doi:10.1016/j.ophtha.2012.10.036 [published Online First: 16  
311 January 2013].
- 312 13 Zayit-Soudry S, Duncan JL, Syed R, et al. Cone structure imaged with adaptive optics scanning laser  
313 ophthalmoscopy in eyes with nonneovascular age-related macular degeneration. *Invest.*  
314 *Ophthalmol. Vis. Sci.* 2013;54(12):7498–509. doi:10.1167/iavs.13-12433 [published Online First: 15  
315 November 2013].
- 316 14 Mrejen S, Sato T, Curcio CA, et al. Assessing the cone photoreceptor mosaic in eyes with  
317 pseudodrusen and soft Drusen in vivo using adaptive optics imaging. *Ophthalmology*  
318 2014;121(2):545–51. doi:10.1016/j.ophtha.2013.09.026 [published Online First: 30 October 2013].

319  
320  
321  
322

323 **FIGURES**

324

325 **Figure 1: Multimodal imaging of four iAMD patients presenting iRORA lesions.**

326 Column 1, Infrared SLO images. OCT B-scan and AOSLO imaging locations are marked  
327 (red=iRORA, blue=eccentricity-matched control region). Column 2, OCT-B scan through the  
328 center of the iRORA lesion. Column 3, magnification of the iRORA lesions marked by the white  
329 rectangle in Column 2. Red arrow heads mark the extent of the lesion as graded from the OCT  
330 scan. Columns 4 and 5 show AOSLO images of iRORA lesions and control regions,  
331 respectively. Arrow heads indicate the corresponding locations after OCT and AOSLO image  
332 registration. In three cases, only a single marker is visible due to the lesion extending beyond  
333 the limited field of view of the AOSLO.

334

335 **Figure 2: Retinal sensitivity at iRORA lesions and control regions in iAMD.**

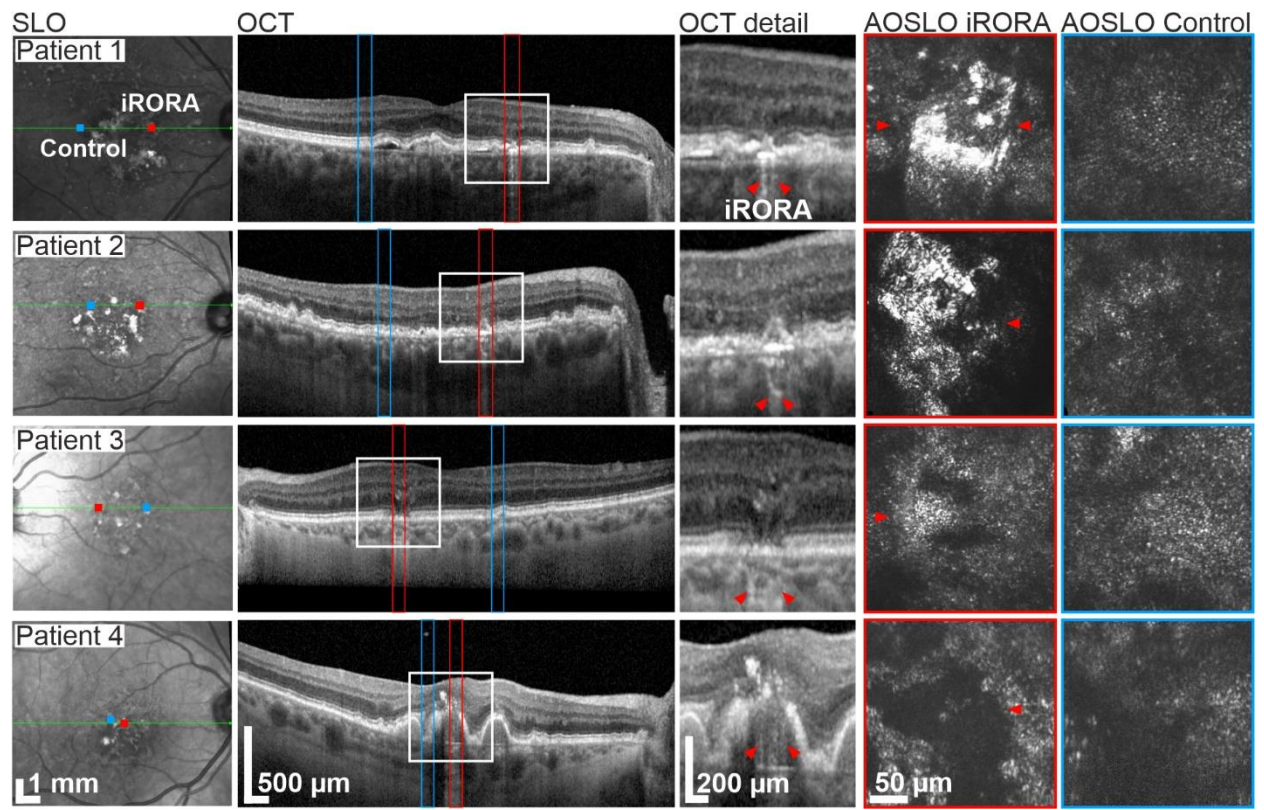
336 **A)** Test spot size comparison between MAIA-MP (achromatic stimulus) and AOSLO-MP (543  
337 nm stimulus within a larger 840 nm raster). **B)** MAIA-MP estimate of retinal sensitivity at the  
338 iRORA lesion (17 dB, red) and control region (27 dB, blue) in patient #3. The marker diameter  
339 corresponds to MAIA-MP stimulus size on the retina. **C) and D)** AOSLO-MP test spot size and  
340 location at the iRORA lesion (C) and control region (D) in patient #3. Sensitivity thresholds were  
341 14 dB and 33.3 dB, respectively. Both areas show patches of normal hexagonally arranged  
342 cone photoreceptors and areas of hyporeflective retina. **E)** Sensitivity thresholds at the iRORA  
343 lesions and control regions for MAIA-MP (patients #1, 3, 4) and AOSLO-MP (patients #1, 2, 3).

344

345

346

347 **Figure 1**

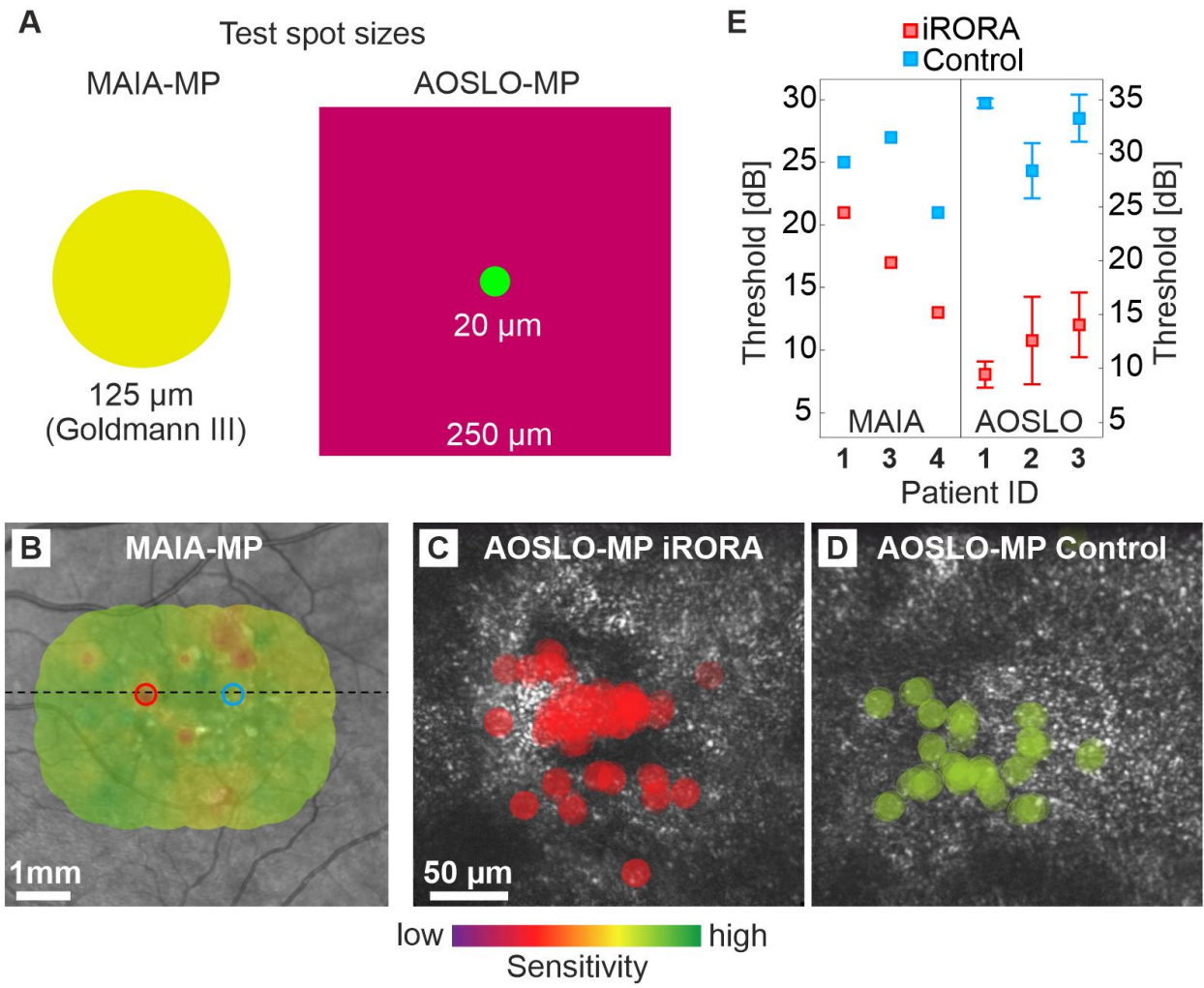


348

349



350 **Figure 2**



351